

Supporting Information

for

Supramolecular polymorphism in aggregates of boron-difluoride complex of *peri*-naphthoindigo via solvent-, and pathway-dependent self-assembly

*Indraneel Debnath,^a Tirupati Roy,^a Jonas Matern,^b Stef Jansen,^{cd} Gustavo Fernández^b and Kingsuk Mahata^{*a}*

^a*Department of Chemistry, Indian Institute of Technology Guwahati, Guwahati -781039, India. mail: kingsuk@iitg.ac.in Fax: (+91) 361-258-2349*

^b*Organisch-Chemisches Institut, Westfälische-Wilhelms Universität Münster, Correnstraße 36, 48149, Münster (Germany).*

^c*Laboratory of Macromolecular and Organic Chemistry, Eindhoven University of Technology, P.O. Box 513, 5600 MB Eindhoven, The Netherlands*

^d*Institute for Complex Molecular Systems (ICMS), Eindhoven University of Technology, P.O. Box 513, 5600 MB Eindhoven, The Netherlands*

Table of contents

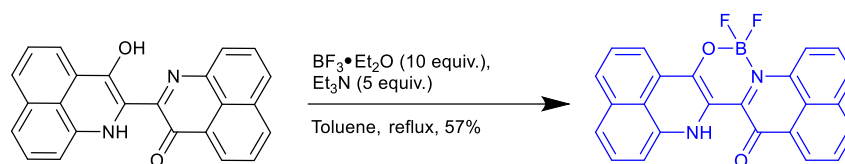
1. Synthesis.....	S2
2. NMR spectroscopy.....	S4
3. Mass spectrum.....	S6
4. UV-vis spectroscopy.....	S7
5. Photoluminescence spectroscopy.....	S21
6. Curve fitting.....	S22
7. FESEM images.....	S25
8. References.....	S26

1. Synthesis

General

All commercially available reagents and solvents were used as received. *perinaphthoindigo* (PNI) was synthesised according to known procedures.¹ Reactions were monitored by analytical thin layer chromatography using commercial aluminum sheets pre-coated with silica gel (silica gel 60 F254) and visualised under 254 nm and 365 nm UV-light. Basic active alumina (70-230 mesh) was used for purification of PNIBF₂. For photophysical studies, HPLC and UV-grade solvents were used. Deuterated solvents for NMR spectroscopy were purchased from Sigma-Aldrich. NMR measurements were done at 293 K on either Bruker AscendTM 400 MHz NMR spectrometer or Bruker Avance III 600 MHz NMR spectrometer using deuterated solvent as the lock and residual solvent as the internal reference. ¹⁹F and ¹¹B NMR data were calibrated using BF₃•Et₂O as external standard. The following abbreviations were utilised to describe peak patterns: s = singlet, d = doublet, t = triplet, q = quartet and m = multiplet. High resolution mass spectrometry (HRMS) measurements were done with Agilent QTOF 6520 mass spectrometer using electrospray ionization (ESI) mode. Absorbance properties were investigated on a Cary 100 UV-vis spectrophotometer, and depending on the concentrations, samples were loaded in quartz UV-cuvettes having either 1 mm or 10 mm path length. Photoluminescence properties were studied on a Horiba Fluoromax-Plus-C fluorimeter using a 10 mm quartz cuvette. Correction of the spectra were done by the correction factor implemented in the software. Infra-red (IR) spectra were collected as a film on KBr using Perkin-Elmer FT-IR spectrometer and frequencies are presented in reciprocal centimeter (cm⁻¹). FESEM images were captured either on a Gemini 300 or on a Sigma 300 FESEM of Zeiss make. Samples were prepared by drop-cast method from the respective solvent system and were left for drying at room temperature for 10-16 h.

Synthesis of PNIBF₂



PNI (50.0 mg, 138 μ mol) was loaded into a round-bottomed flask and dissolved in 10 mL of toluene. Triethylamine (95.0 μ L, 689 μ mol) was added to the solution and stirred at 90 °C for a period of 10 minutes. To the hot solution BF₃·Et₂O (170 μ L, 1.38 mmol) was added, and the mixture was refluxed for overnight. After cooling down the reaction mixture to room temperature, the organic solvent was evaporated to dryness under reduced pressure. The solid was then dissolved in a mixture of 1:1 (v/v) chloroform-THF and passed through a pad of basic alumina. After removal of the organic solvents under reduced pressure, the solid was washed with hexane (3 x 10 mL) and methanol (3 x 10 mL). The BF₂-coordinated compound was dried and used for investigation without doing further purification. Yield = 32.0 mg (57%); ¹H-NMR (600 MHz, CDCl₃, 293 K) δ 8.78 (d, ³J = 7.8 Hz, 1H), 8.67 (d, ³J = 7.2 Hz, 1H), 8.33 (d, ³J = 7.8 Hz, 1H), 8.30 (d, ³J = 7.2 Hz, 1H), 8.17 (d, ³J = 7.8 Hz, 1H), 7.92 (d, ³J = 7.2 Hz, 1H), 7.81-7.86 (m, 4H), 7.68-7.74 (m, 2H), 7.49 (s, 1H) ppm; ¹⁹F NMR (376 MHz, CDCl₃, 293 K) δ -130.7 (q, ¹J_{B-F} = 34.6 Hz, 2F) ppm; ¹¹B NMR (128 MHz, CDCl₃, 293 K) (t, ¹J_{B-F} = 34.6 Hz, 1B) ppm; HRMS (ESI) *m/z* calcd for [M-2F + Na]⁺ 395.0967, found: 395.1062; IR (KBr) 764, 775, 808, 826, 841, 903, 934, 990, 1021, 1072, 1112, 1178, 1195, 1225, 1264, 1295, 1345, 1372, 1392, 1423, 1467, 1503, 1524, 1550, 1595, 1658, 2851, 2921, 3061, 3432. cm⁻¹; UV/vis (CHCl₃) λ_{max} /nm (ϵ /M⁻¹cm⁻¹) 659 (43 255), 606 (29530).

2. NMR spectra

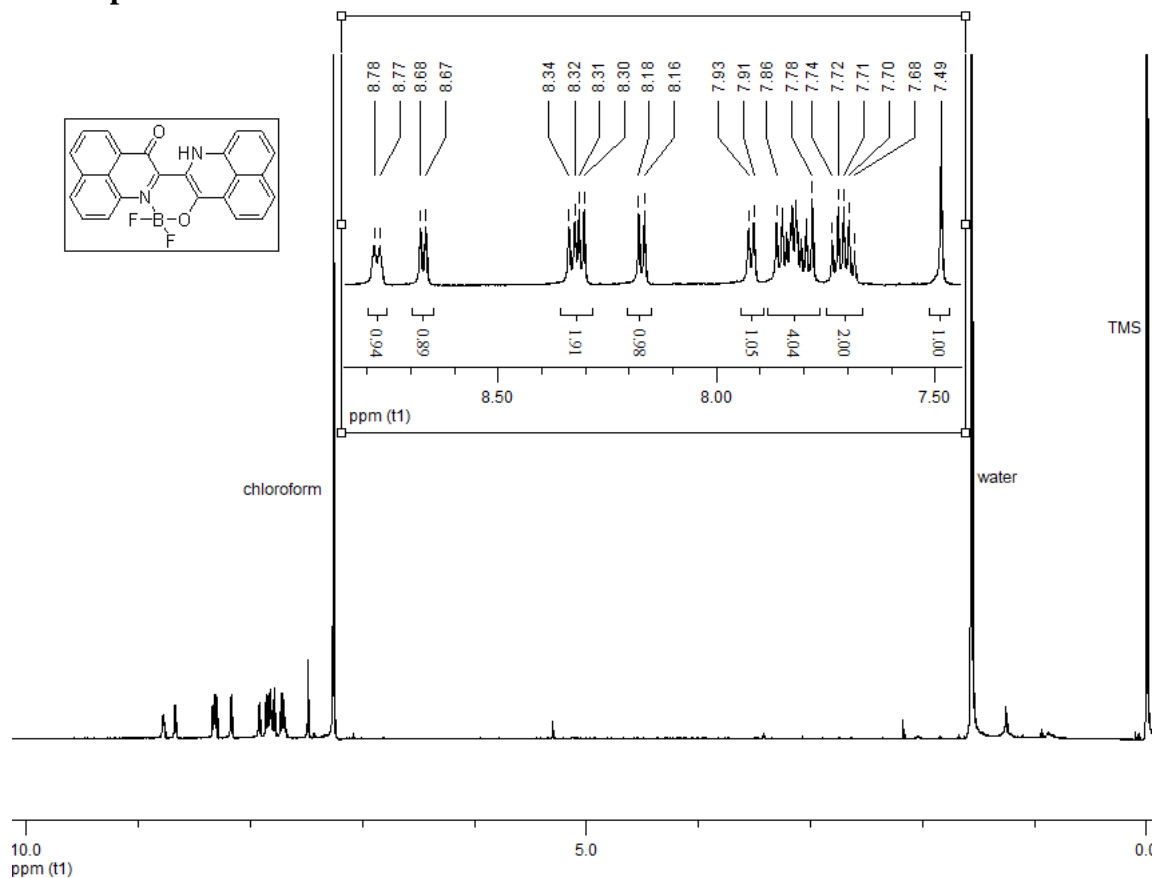


Figure S1. ^1H NMR spectrum of PNIBF₂ (600 MHz, CDCl₃, 293 K).

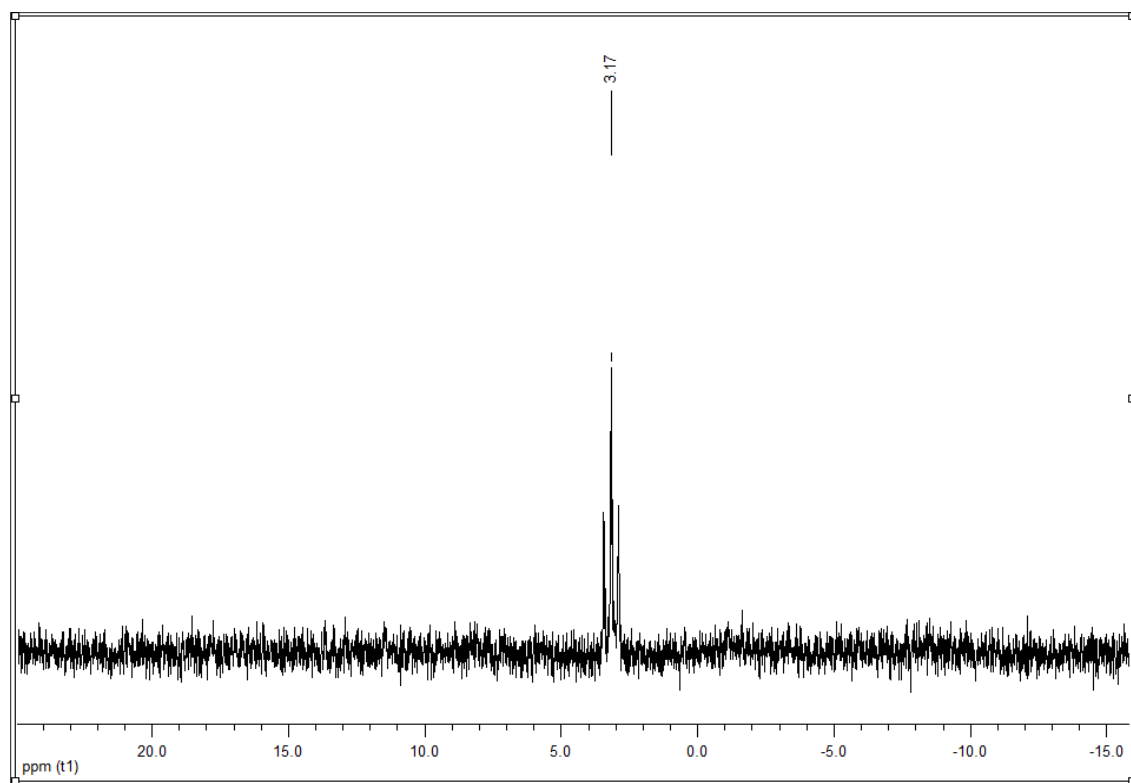


Figure S2. ^{11}B NMR spectrum of PNIBF₂ (128 MHz, CDCl₃, 293 K).

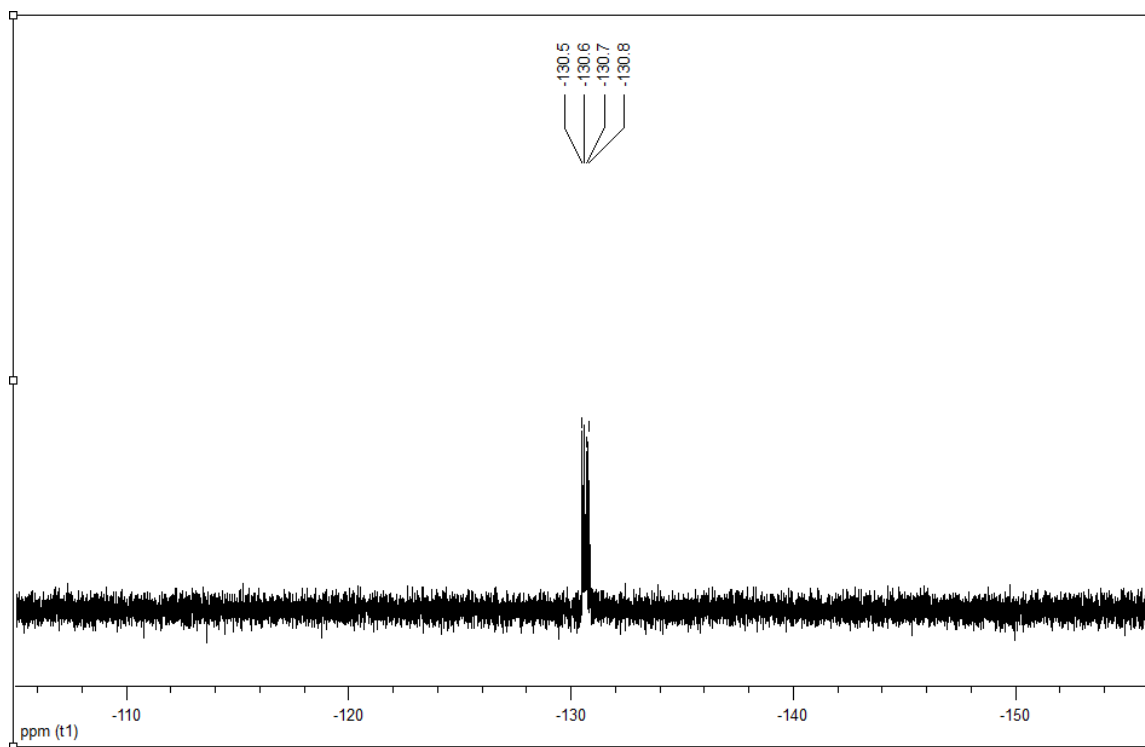


Figure S3. ^{19}F NMR spectrum of PNIBF₂ (376 MHz, CDCl₃, 293 K)

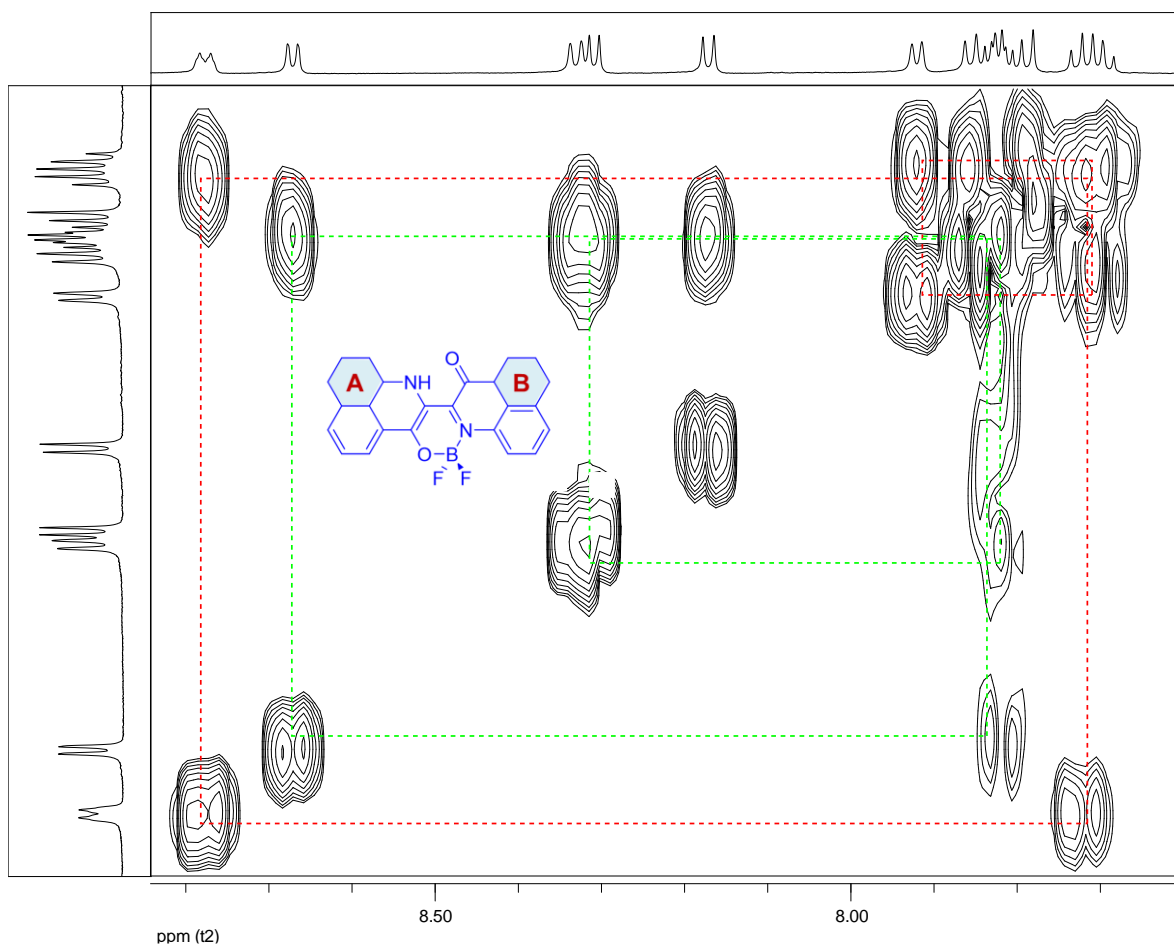


Figure S4. ^1H - ^1H COSY (400 MHz, 293 K) spectrum of PNIBF₂ in CDCl₃. Connectivity of the protons of A and B rings are shown in the spectrum.

3. Mass spectrum

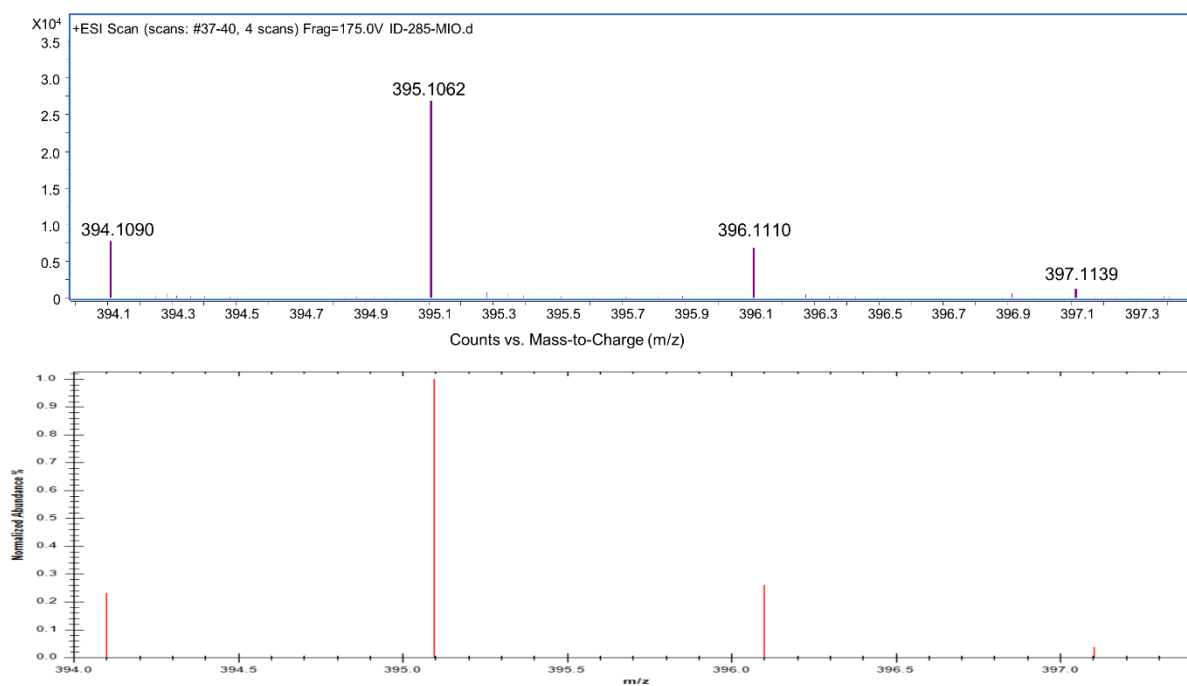


Figure S5. HRMS (ESI) spectrum (acetonitrile) of $[\text{PNIBF}_2\text{-2F} + \text{Na}]^+$ along calculated isotopic distribution (below, red).

4. UV-vis spectroscopy

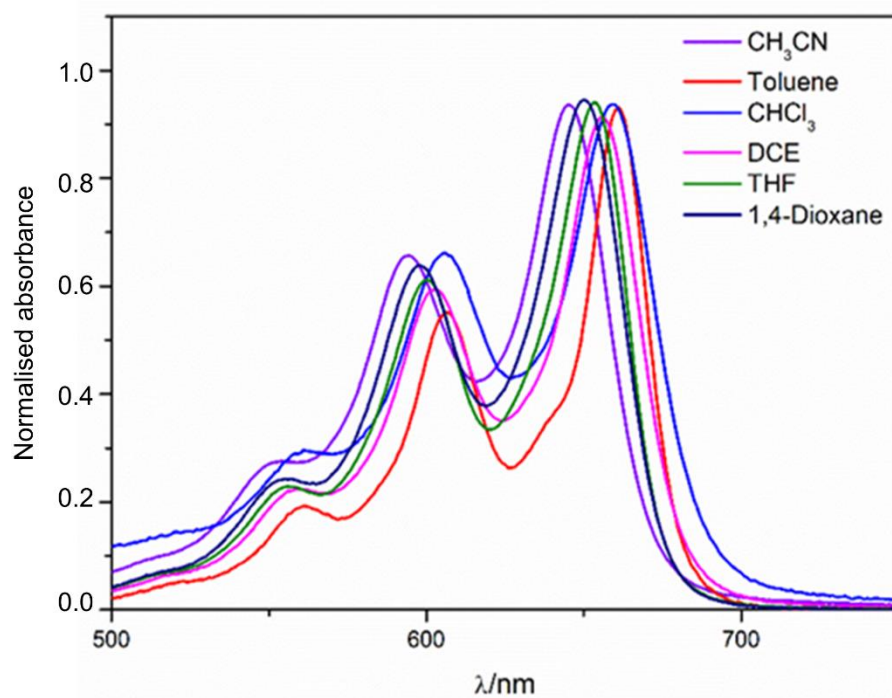


Figure S6. Absorption spectra (293 K) of PNIBF₂ in various solvents. Spectrum in toluene showed additional shoulder at around 635 nm, suggesting its aggregation behaviour in non polar solvent.

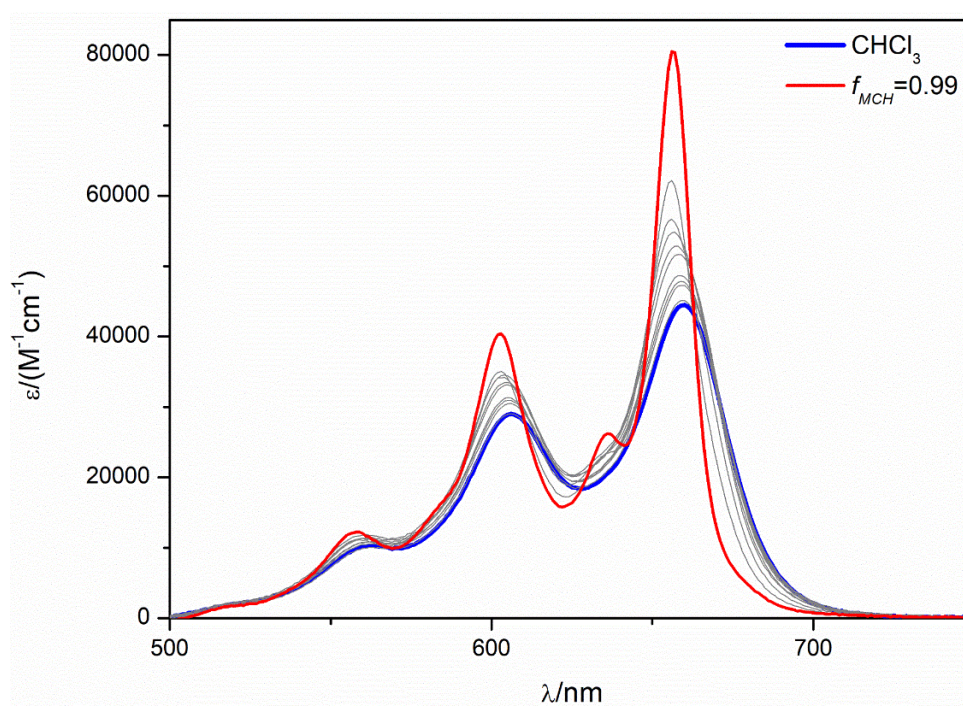


Figure S7. Absorption spectra (5 μ M, 293 K) of PNIBF₂ in chloroform (blue) and in various v/v mixture of MCH-CHCl₃.

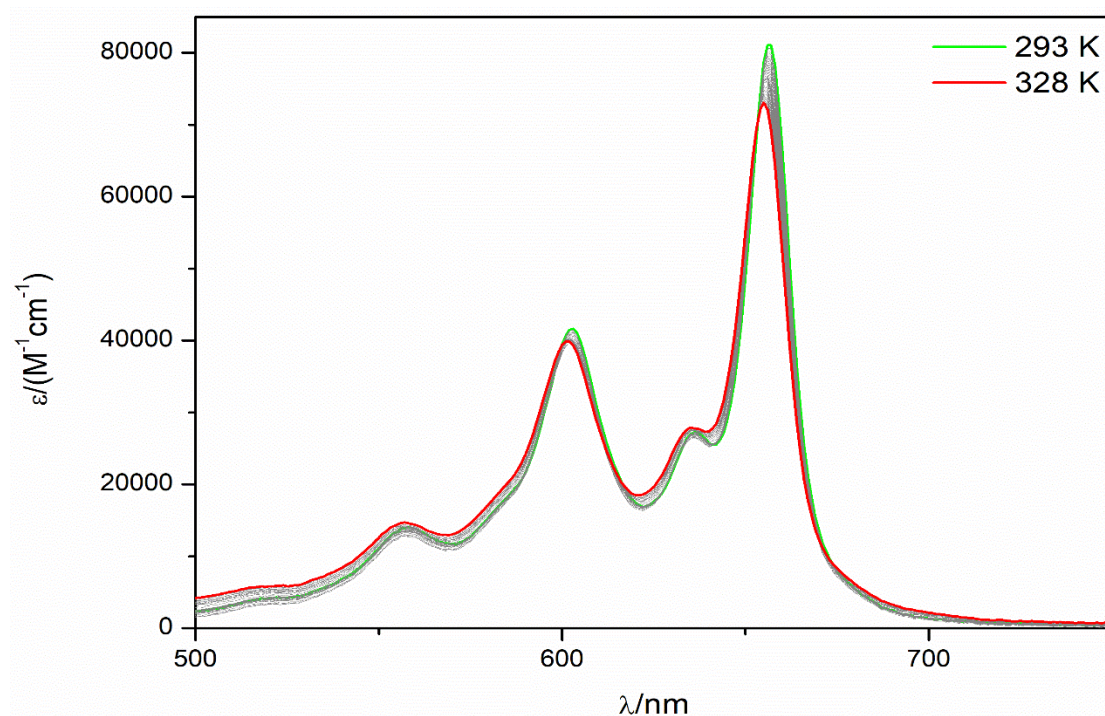


Figure S8. Variable temperature absorption spectra of PNIBF₂ in a 99/1 (v/v) mixture of MCH/CHCl₃ at a concentration of 5 μM.

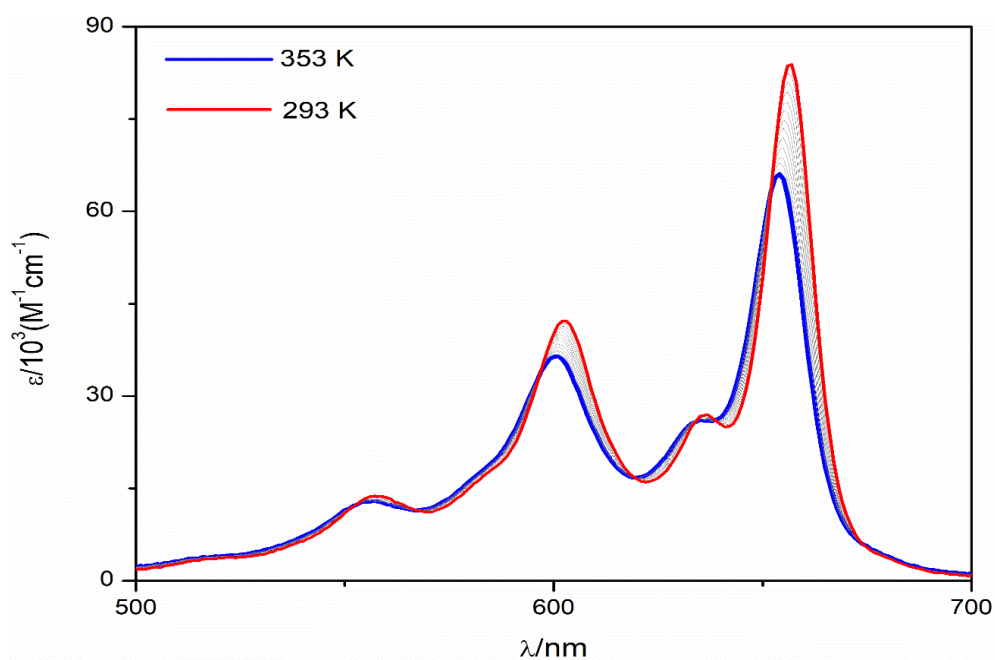


Figure S9. Absorption spectra of PNIBF₂ ($c \approx 5 \mu\text{M}$) in DCE-MCH (v/v=1:99) at various temperatures. Higher molar extinction coefficient at room temperature confirmed aggregation.

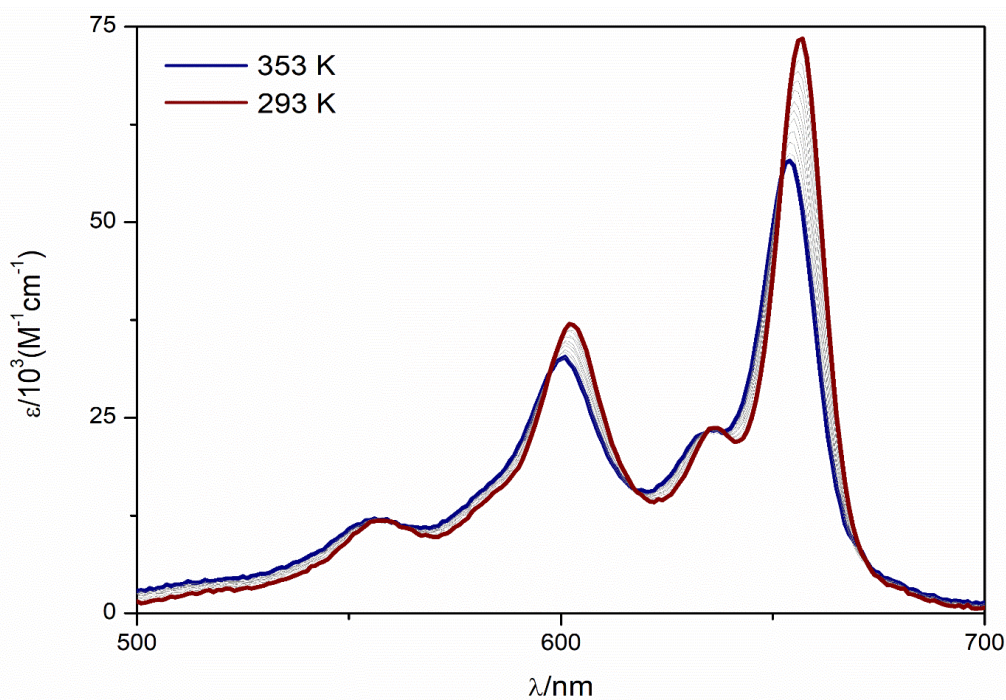


Figure S10. Absorption spectra of PNIBF₂ ($c \approx 2.5 \mu\text{M}$) in DCE-MCH (v/v=1:99) at various temperatures. Higher molar extinction coefficient at room temperature confirmed aggregation.

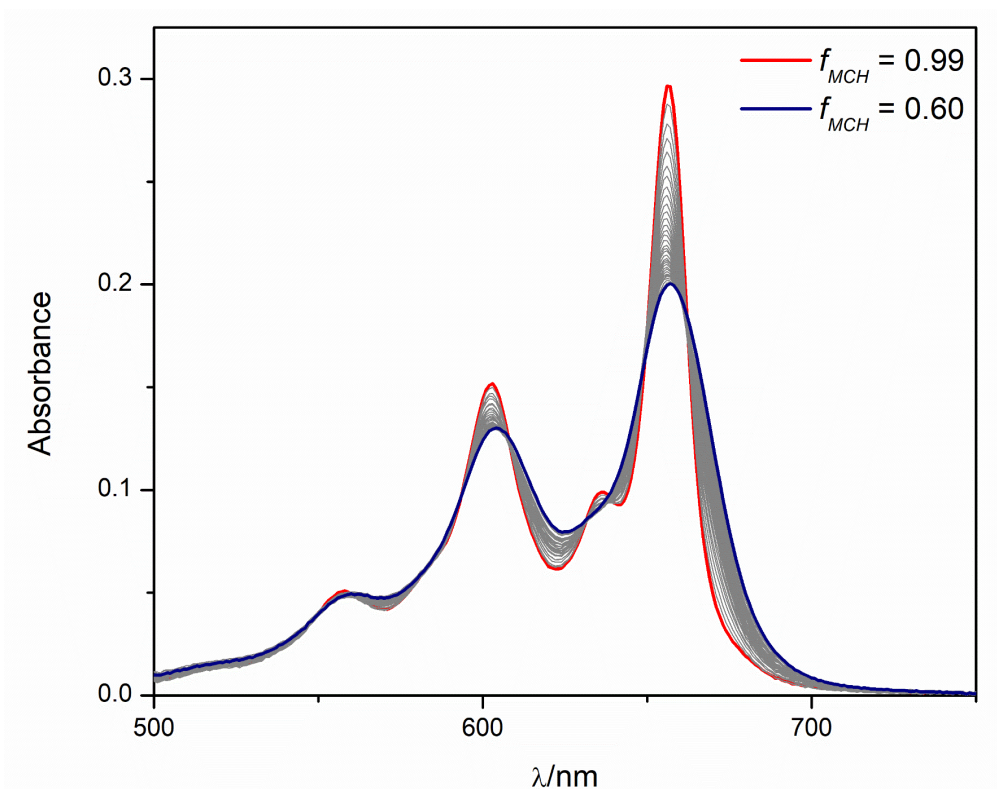


Figure S11. Absorption spectra (3.5 μM , 293 K) of PNIBF₂ in various v/v mixtures of MCH-CHCl₃. The aggregate (red line) in 99/1 (v/v) MCH-CHCl₃ gradually denatures with decreased volume fraction of MCH.

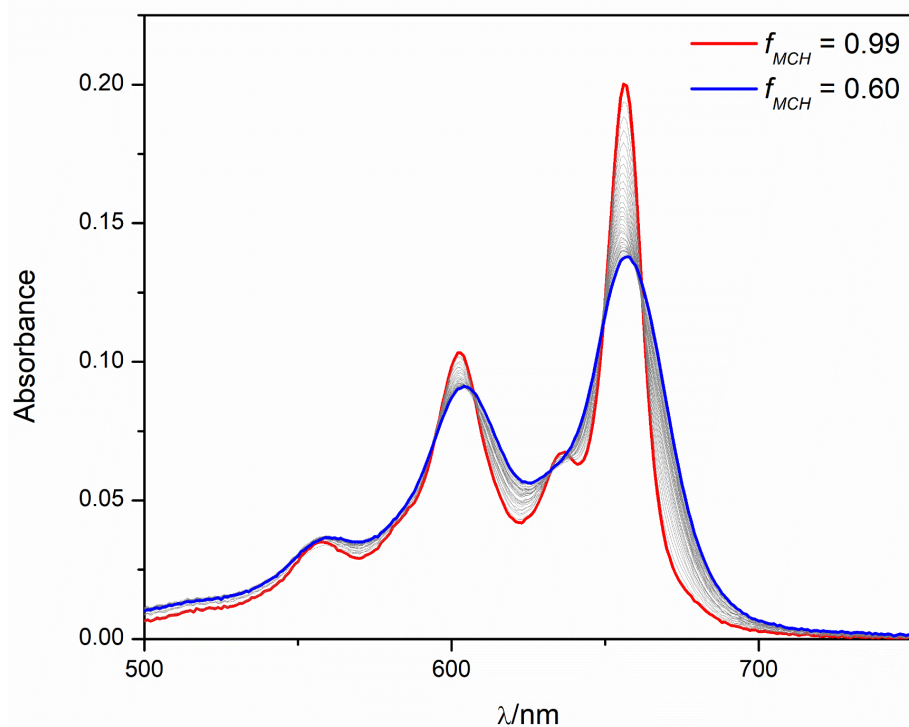


Figure S12. Absorption spectra (2.5 μ M, 293 K) of PNIBF₂ in various v/v mixture of MCH-CHCl₃. The aggregate (red line) in 99/1 (v/v) MCH-CHCl₃ gradually denaturates with decreased volume fraction of MCH.

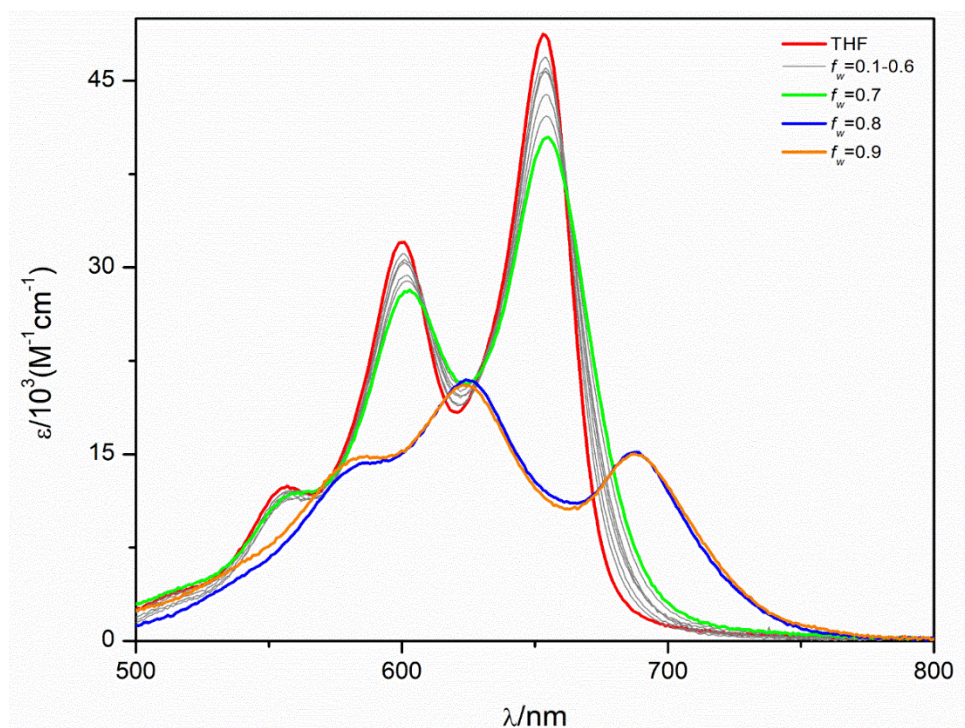


Figure S13. Absorbance spectra of PNIBF₂ ($c \approx 5 \mu$ M) in water-THF mixtures at 293 K. f_w = fraction of water in the mixture.

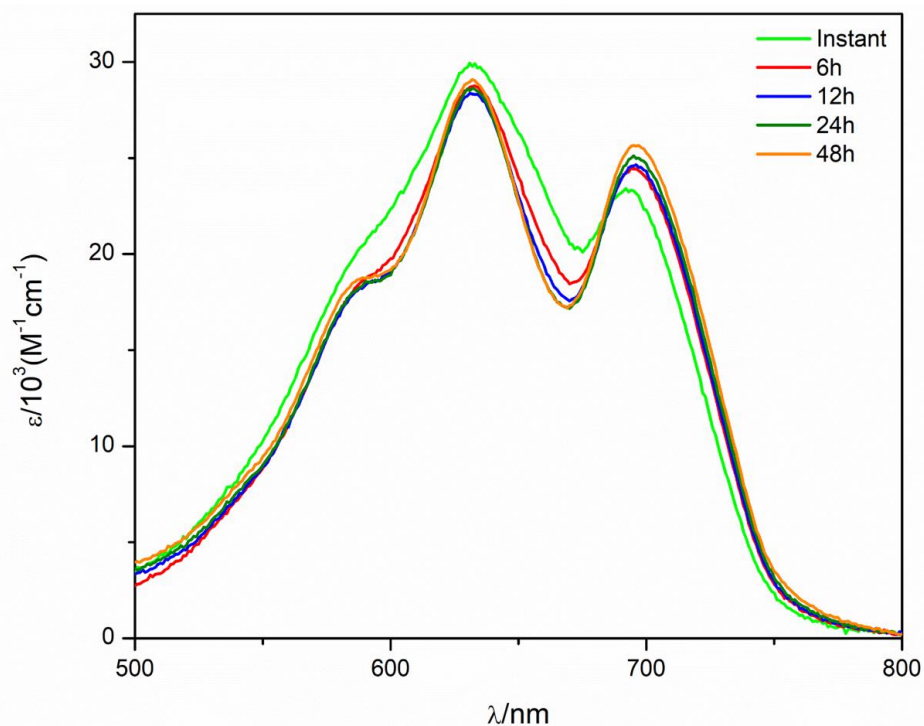


Figure S14. Absorption spectra of PNIBF₂ ($c \approx 5 \mu\text{M}$) in a 76/24 (v/v) water-THF mixtures after different time intervals. Completion of **Agg2** requires at least 6 h after mixing. After that, there was no change in absorption maxima. Variation in relative intensities of $A_{0,0}/A_{0,1}$ with time was due to increase in size of the aggregates.

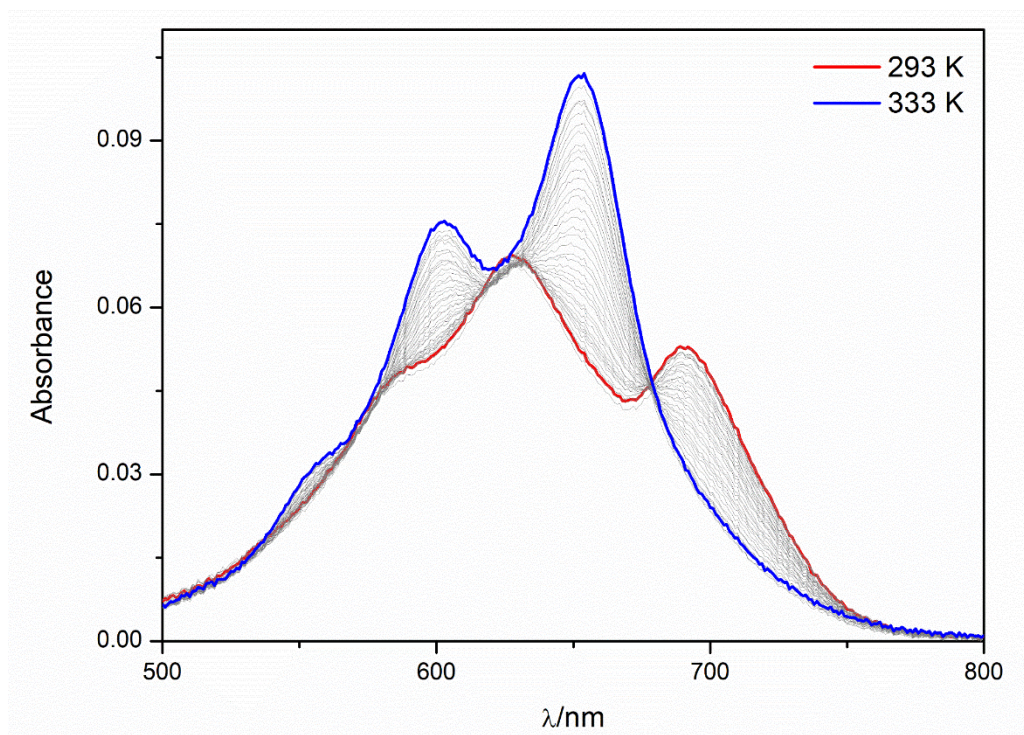


Figure S15. Dis-assembly of **Agg2** in a 76/24 (v/v) mixture of water/THF at a concentration of $3.0 \mu\text{M}$. Gradual dissociation was observed upon heating the solution.

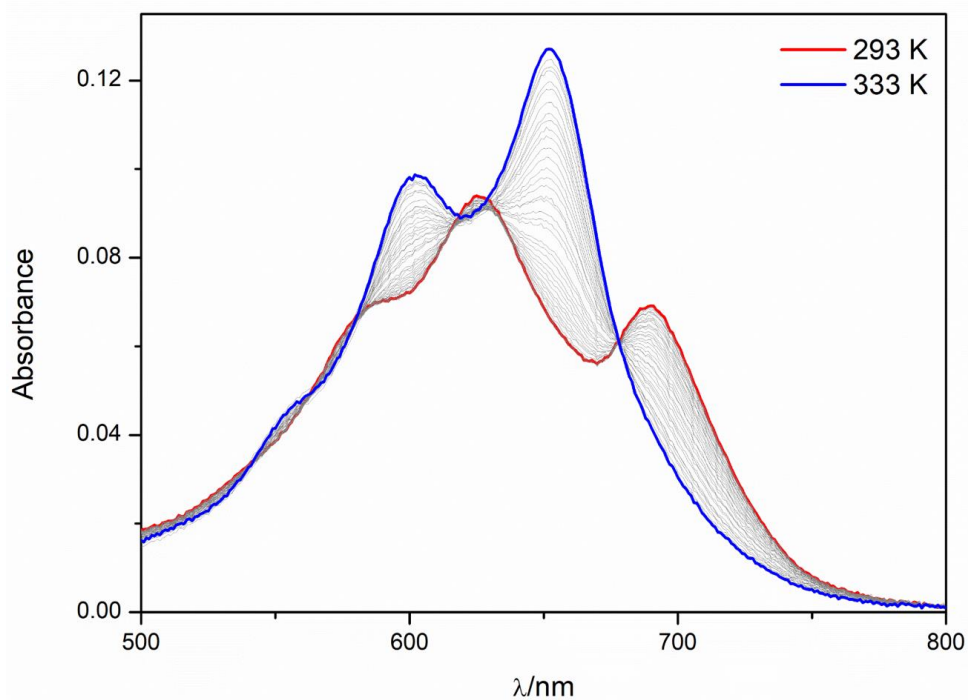


Figure S16. Dis-assembly of **Agg2** in a 76/24 (v/v) mixture of water/THF at a concentration of 4.0 μM. Gradual dissociation was observed upon heating the solution.

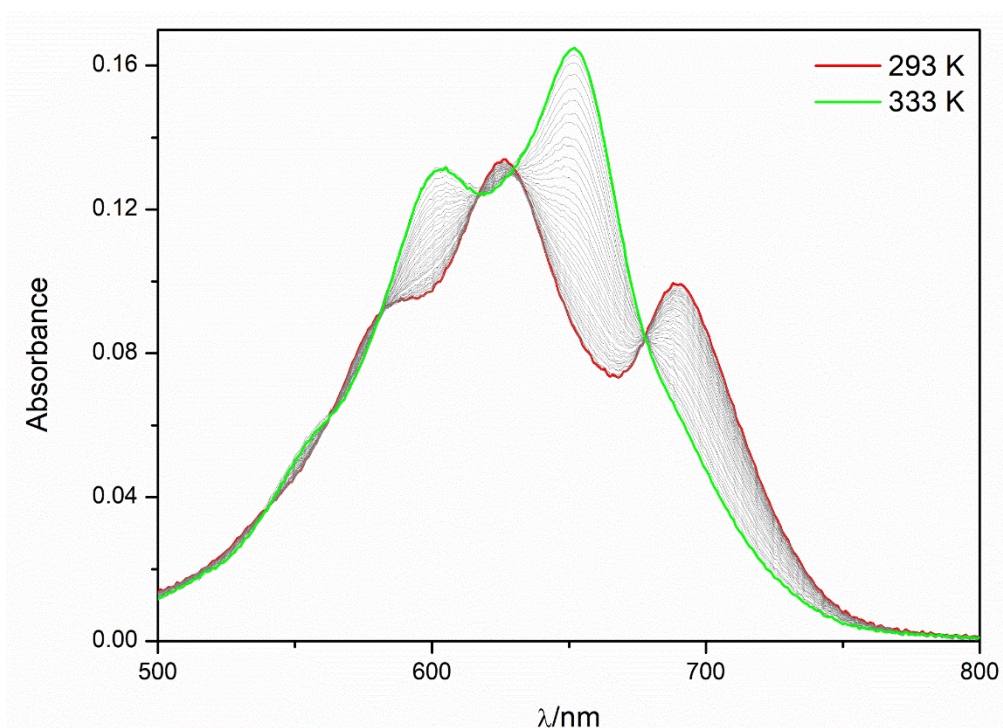


Figure S17. Dis-assembly of **Agg2** in a 76/24 (v/v) mixture of water/THF at a concentration of 6.0 μM. Gradual dissociation was observed upon heating the solution.

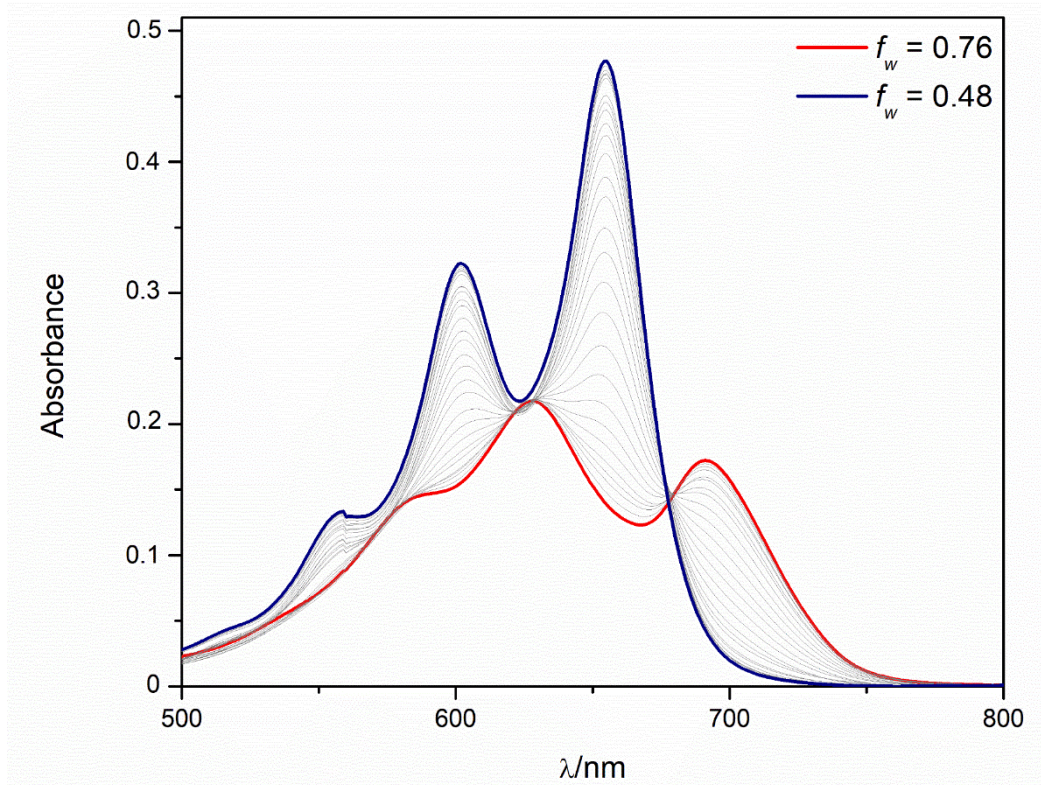


Figure S18. Denaturation of **Agg2** (293 K, 10 μ M) by mixing equimolar mixture of **Agg2** in 76/24 (v/v) mixture of water-THF and PNIBF₂ in THF.

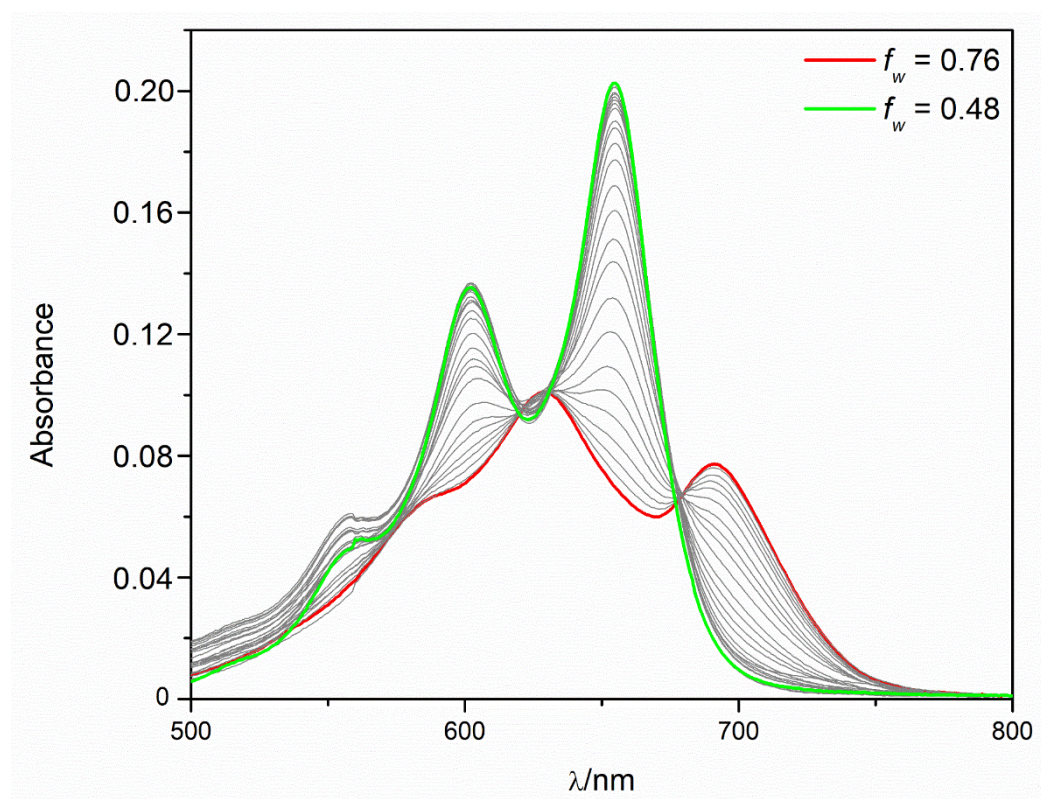


Figure S19. Denaturation of **Agg2** (293 K, 4.0 μ M) by mixing equimolar mixture of **Agg2** in 76/24 (v/v) mixture of water-THF and PNIBF₂ in THF.

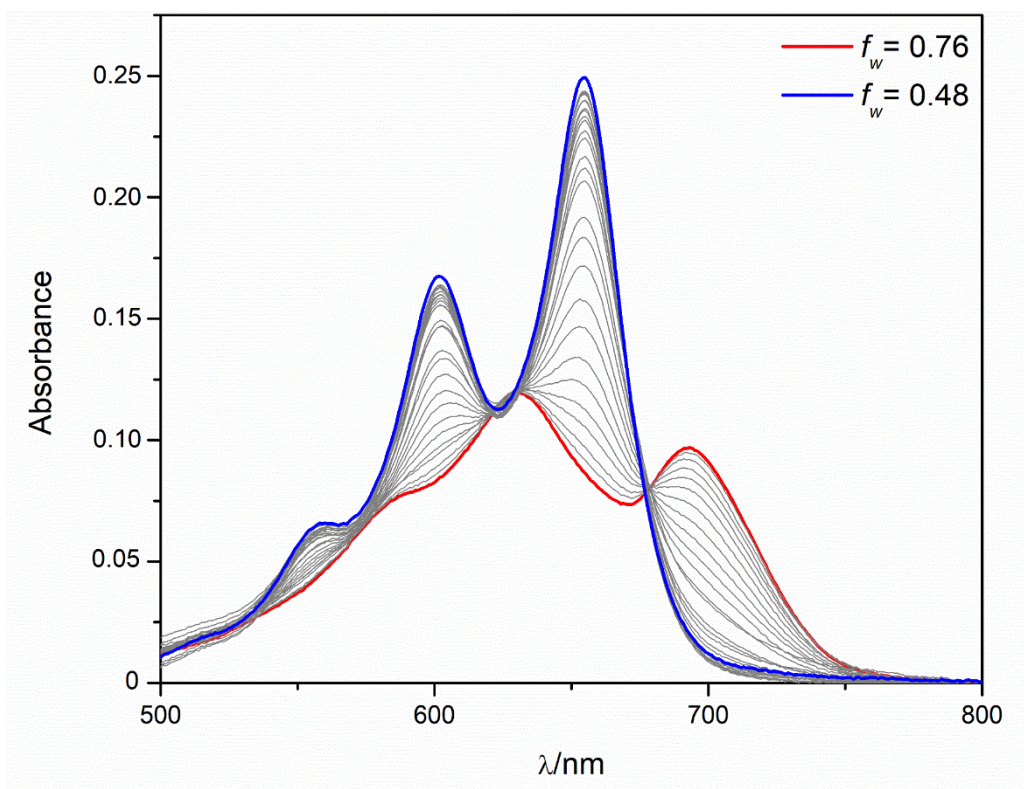


Figure S20. Denaturation of **Agg2** (293 K, 5.0 μM) by mixing equimolar mixture of **Agg2** in 76/24 (v/v) mixture of water-THF and PNIBF_2 in THF.

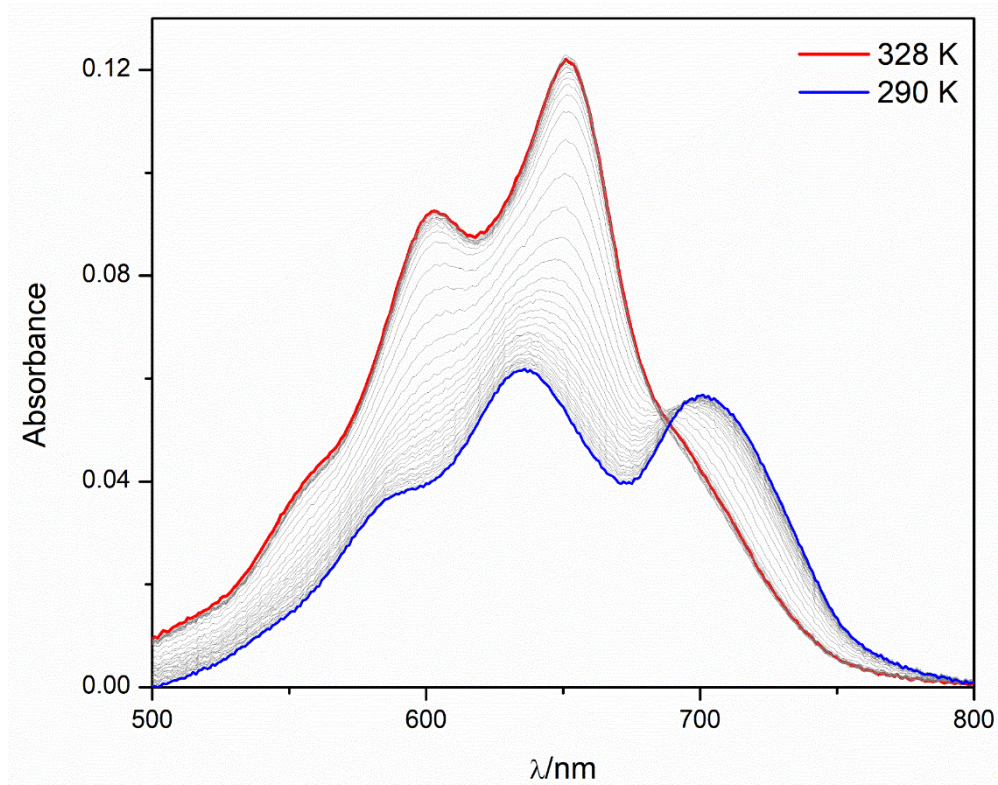


Figure S21. Self-assembly of **Agg3** in a 76/24 (v/v) mixture of water-THF at a concentration of 4.0 μM .

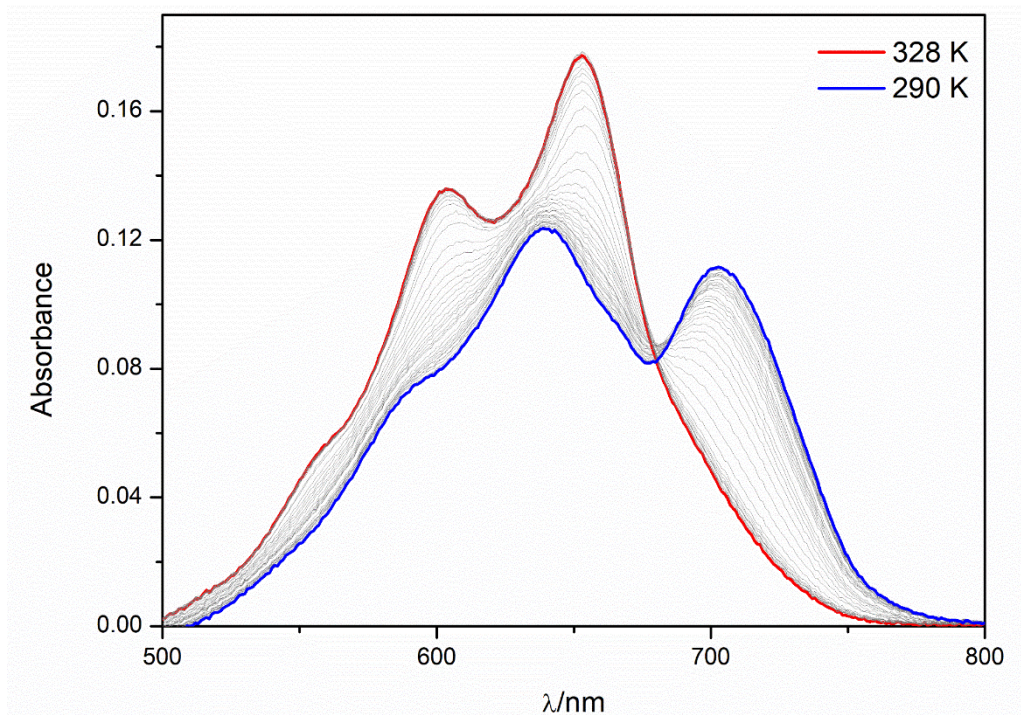


Figure S22. Self-assembly of **Agg3** in a 76/24 (v/v) mixture of water-THF at a concentration of 6.0 μM.

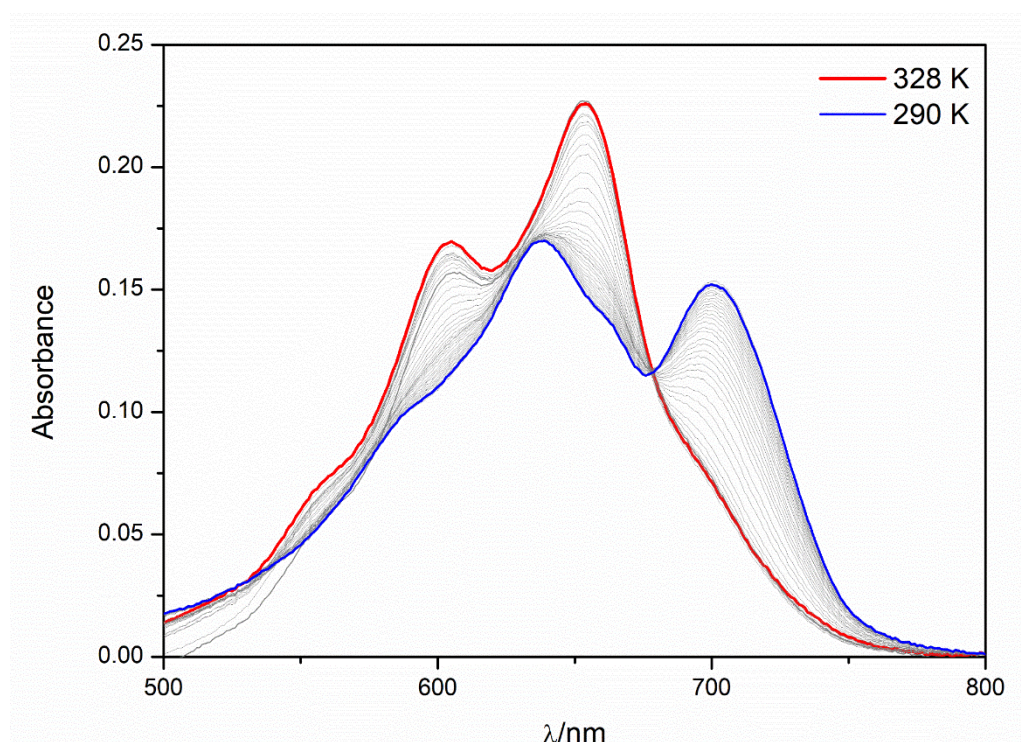


Figure S23. Self-assembly of **Agg3** in a 76/24 (v/v) mixture of water-THF at a concentration of 7.0 μM.

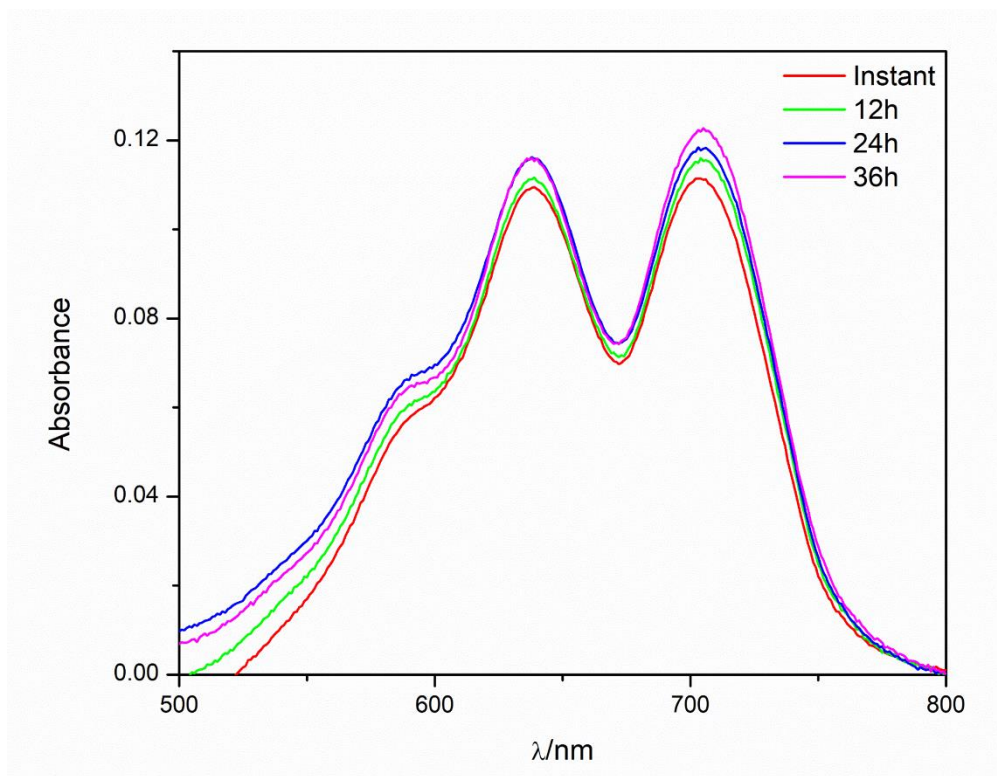


Figure S24. Time dependent absorption spectra (293 K, 5.0 μM .) of **Agg3** in a 76/24 (v/v) mixture of water-THF.

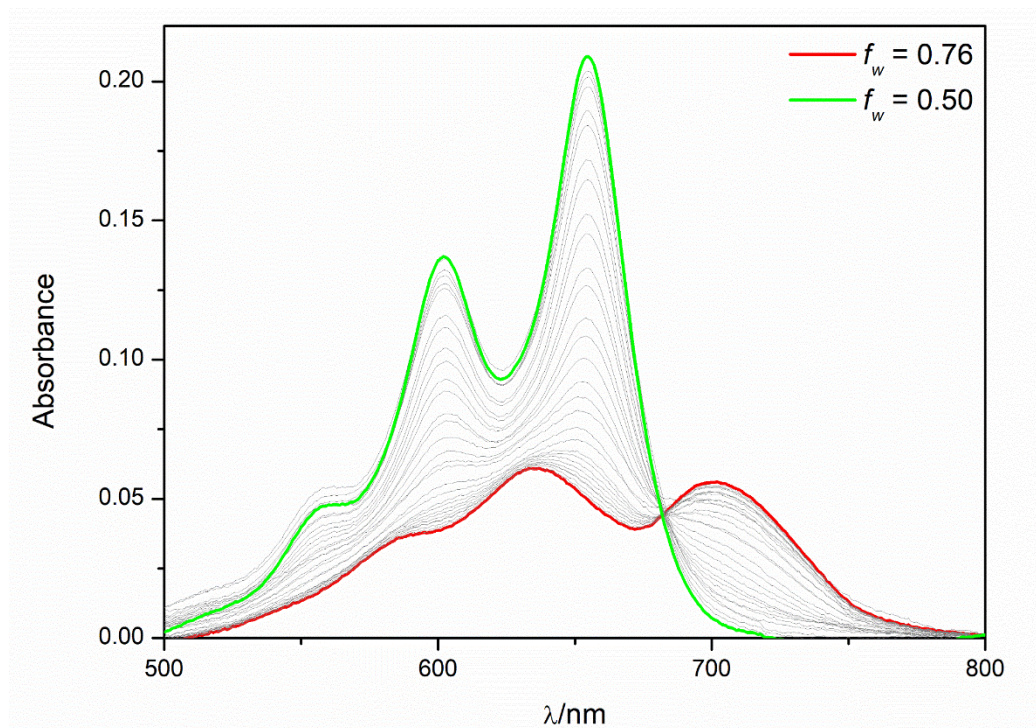


Figure S25. Denaturation of **Agg3** (293 K, 4.0 μM) by mixing equimolar mixture of **Agg3** in 76/24 (v/v) mixture of water-THF and PNIBF₂ in THF.

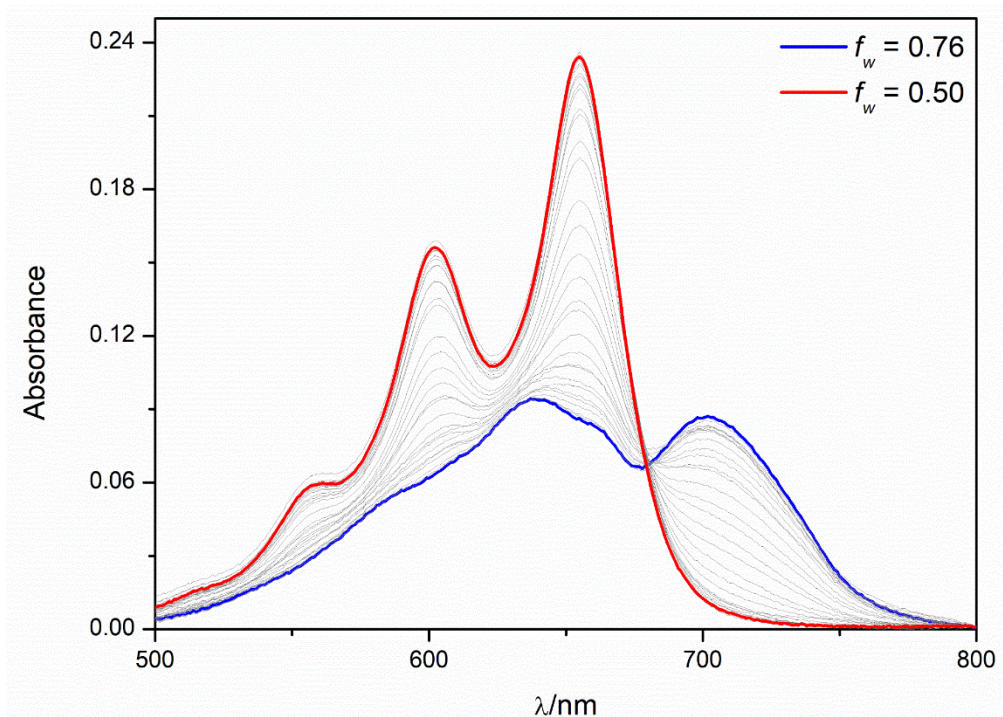


Figure S26. Denaturation of **Agg3** (293 K, 5.0 μM) by mixing equimolar mixture of **Agg3** in 76/24 (v/v) mixture of water-THF and PNIBF₂ in THF.

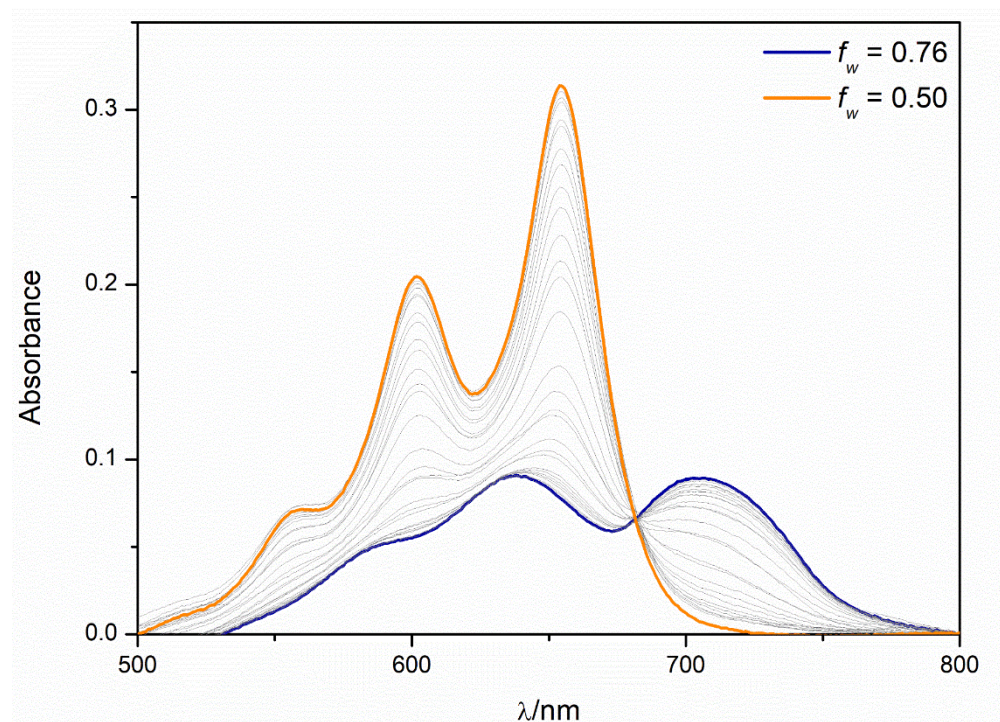


Figure S27. Denaturation of **Agg3** (293 K, 6.0 μM) by mixing equimolar mixture of **Agg3** in 76/24 (v/v) mixture of water-THF and PNIBF₂ in THF.

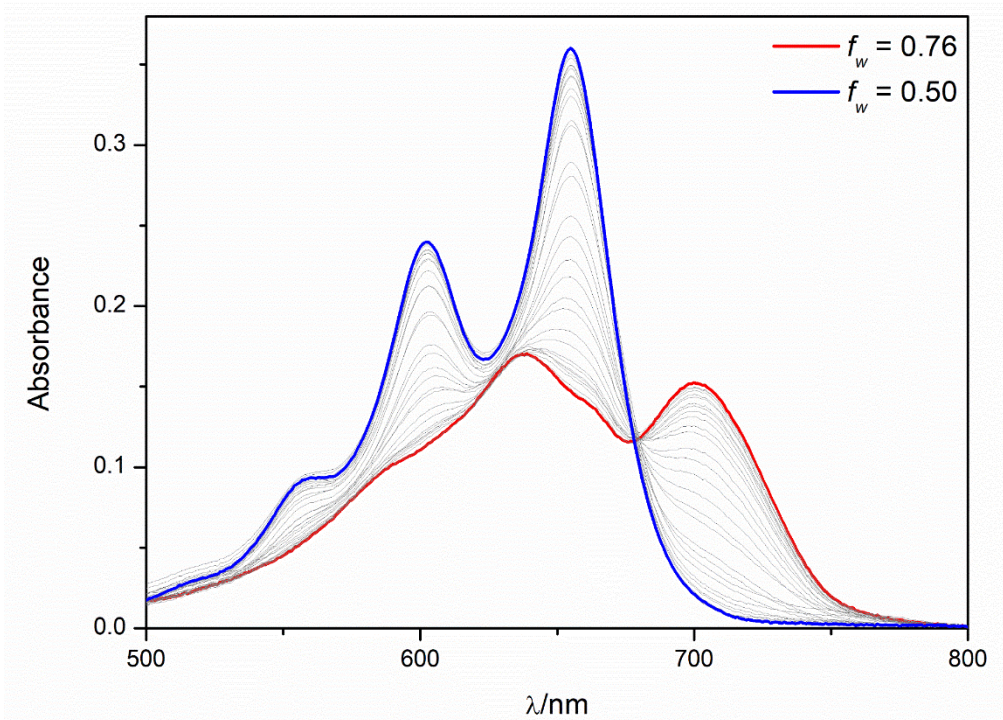


Figure S28. Denaturation of **Agg3** (293 K, 7.0 μM) by mixing equimolar mixture of **Agg3** in 76/24 (v/v) mixture of water-THF and PNIBF_2 in THF.

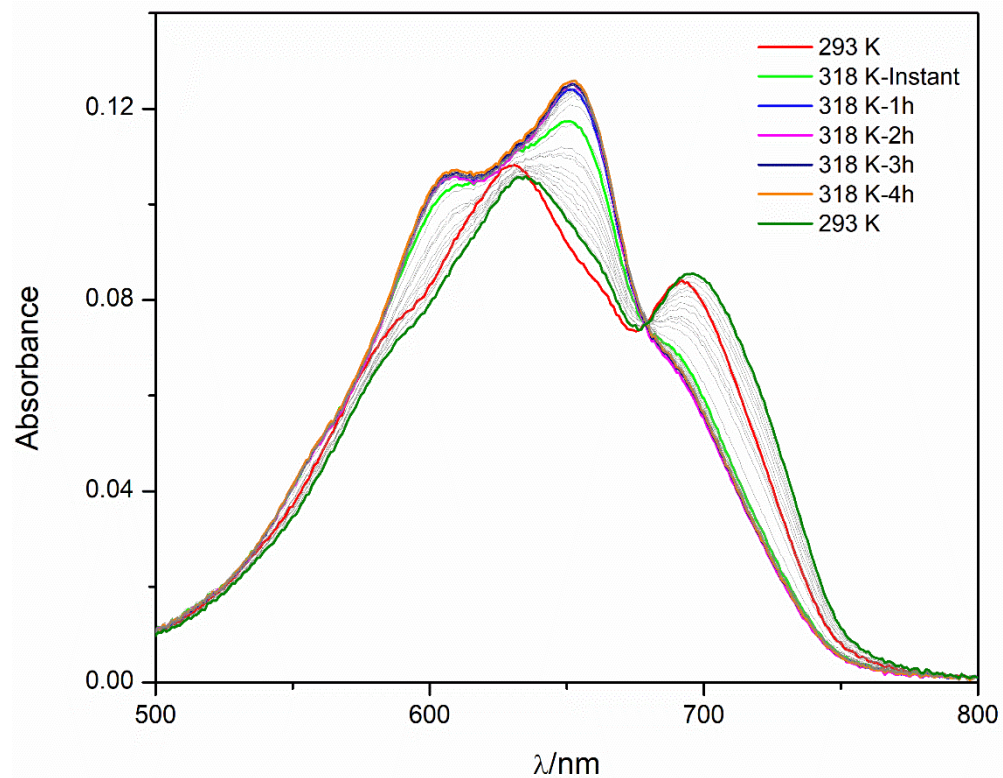


Figure S29. Temperature dependent absorbance spectra ($c \approx 5.0 \mu\text{M}$) of **Agg2** in a 76/24 (v/v) mixture of water-THF at various temperatures. After preparation, the aggregate was kept at 318 K for 4 h, and subsequently cooled down to 293 K. After partial dis-assembly (within 1 h), the spectra remained invariant.

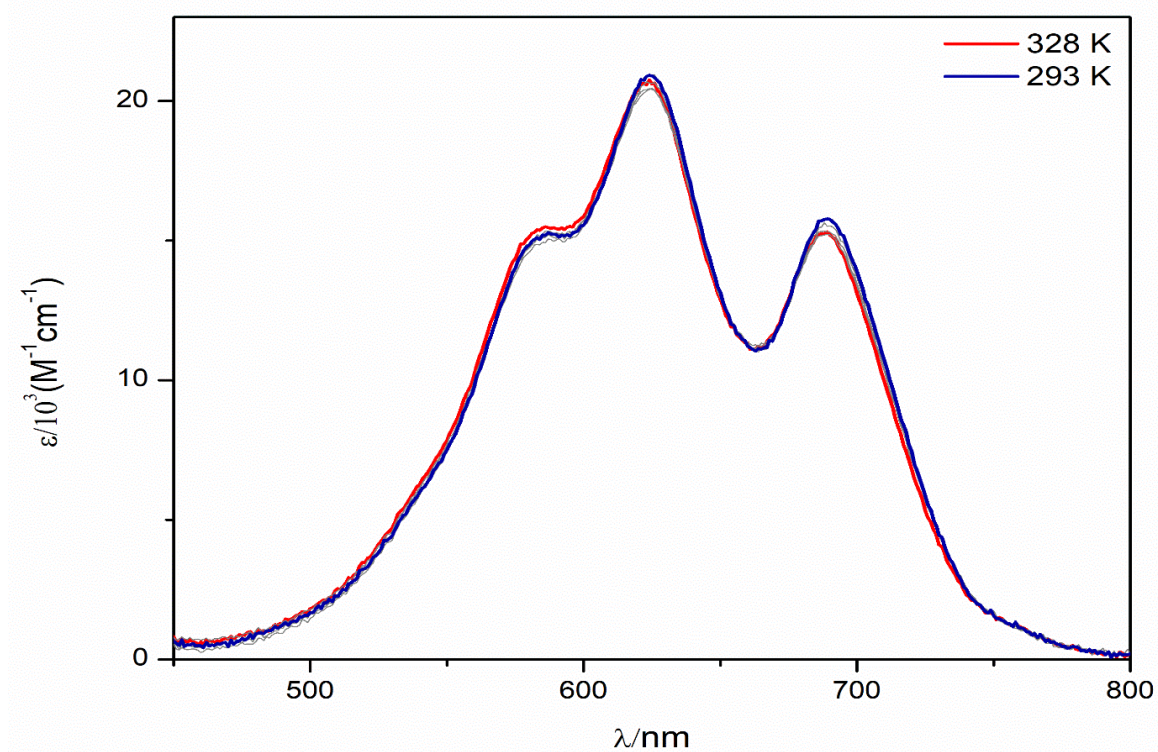


Figure S30. Absorbance spectra of PNIBF₂ ($c \approx 5 \mu\text{M}$) in a 95/5 (v/v) water-THF mixtures at various temperatures. The aggregate did not dissociate and remained stable even at elevated temperatures.

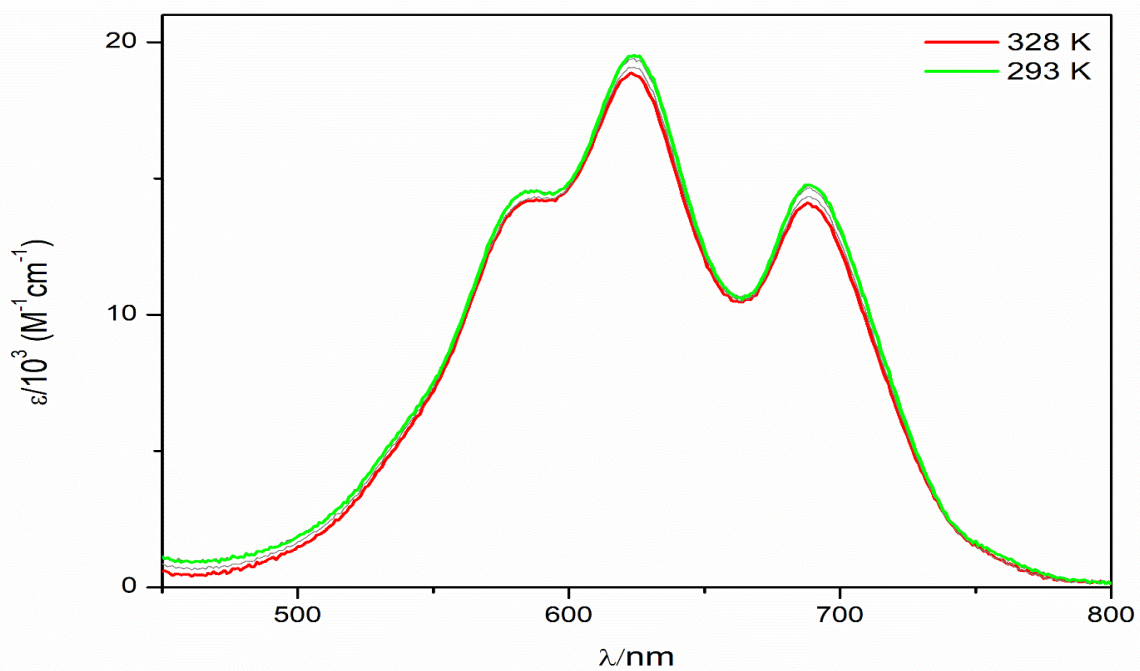


Figure S31. Absorbance spectra of PNIBF₂ ($c \approx 7.5 \mu\text{M}$) in a 95/5 (v/v) water-THF mixtures at various temperatures. The aggregate did not dissociate and remained stable even at elevated temperatures.

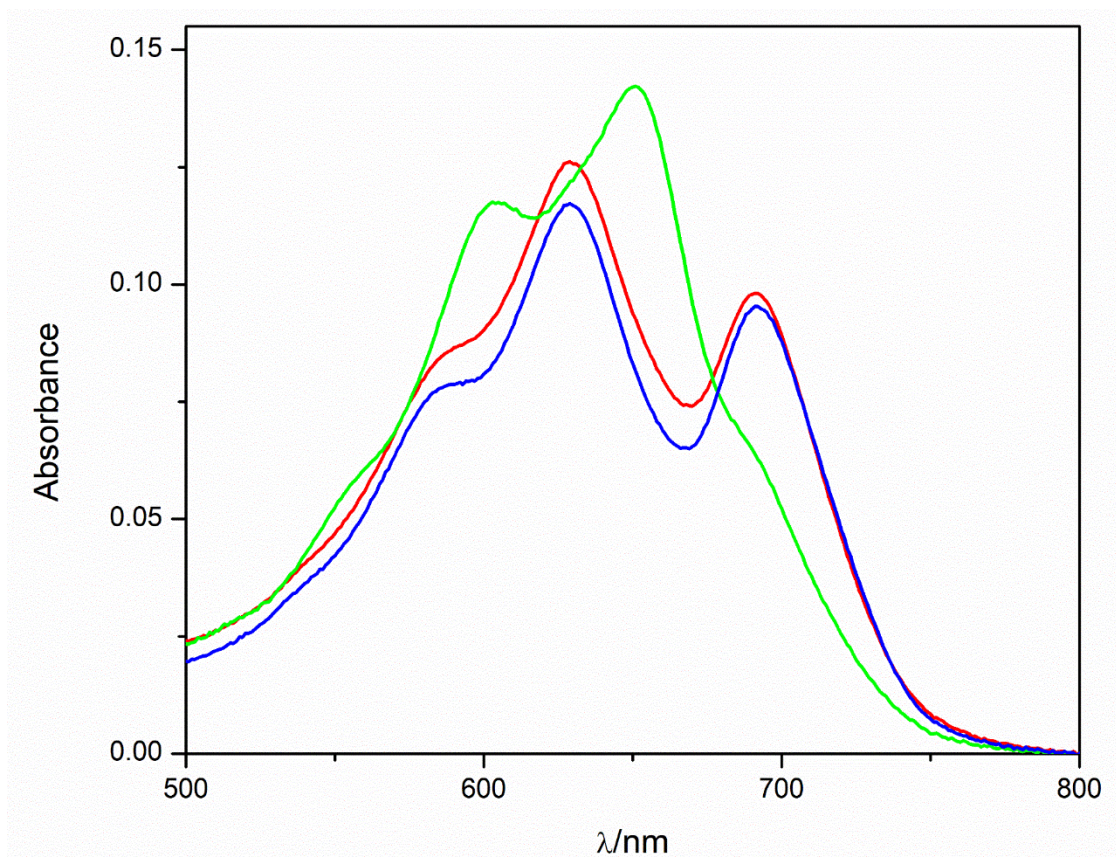


Figure S32. Absorption spectra of freshly prepared **Agg2** (red), monomer (green), and regenerated **Agg2** (blue). via fast cooling. After self-assembly of PNIBF₂ into **Agg2** via dispersion method (red spectrum), the solution was heated to 328 K (green spectrum). The warm solution was then cooled down quickly by placing the container inside ice-cold water (278 K) for 10 min. The spectrum was recorded again at 293 K (blue spectrum). The spectra of freshly prepared **Agg2** and regenerated **Agg2** were found to be similar.

5. Photoluminescence spectroscopy

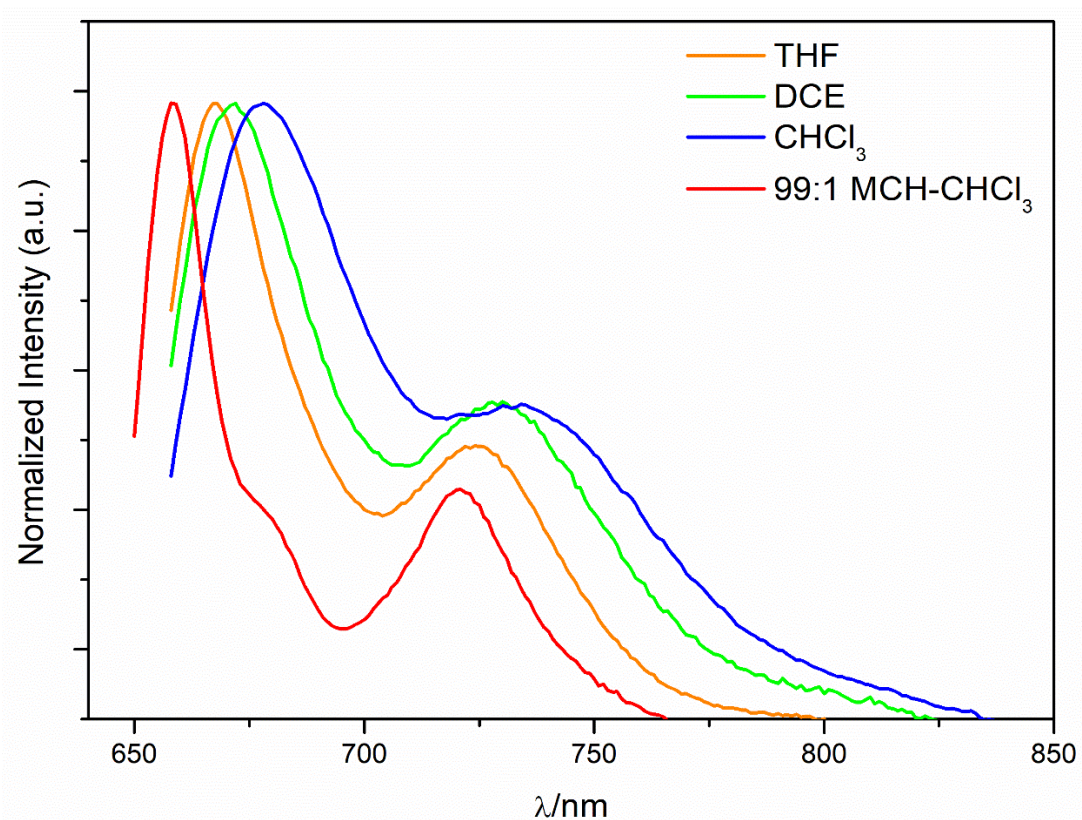


Figure S33. Photoluminescence spectra of PNIBF₂ in various solvents. Samples were excited at respective absorption maxima. The dye shows monomeric emission in THF, chloroform and DCE. However, in a 99/1 (v/v) mixture of MCH-CHCl₃, the spectral feature resembles of aggregate, marked by additional shoulder at 675 nm.

6. Curve fitting²

Agg2 via heating

Method 1: Individual fits + averaging

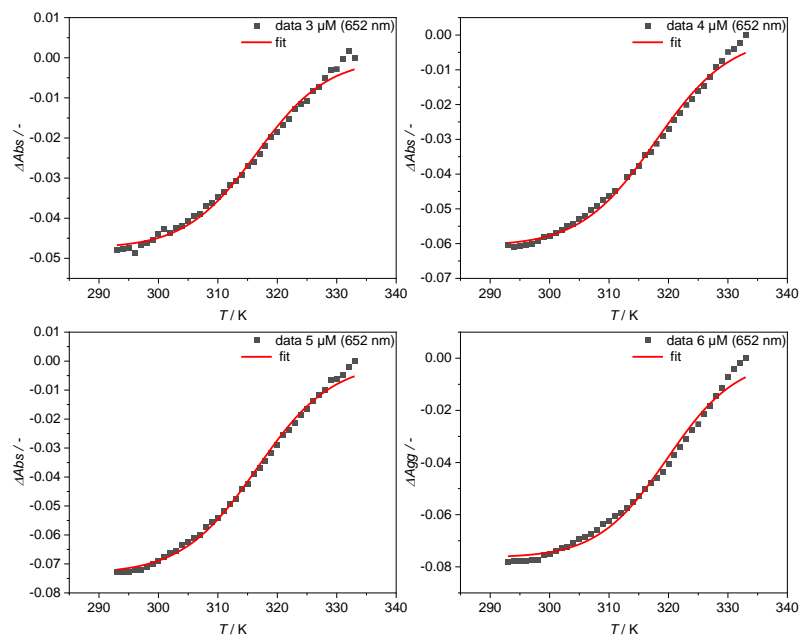


Figure S34. Fit curves for the temperature-induced disassembly of **Agg2** extracted from the absorption data for different concentrations and corresponding individual fit curves.

Table S1. Thermodynamic parameters derived from individual fitting via heating **Agg2**.

dataset	ΔH / kJmol ⁻¹	ΔS / Jmol ⁻¹	ΔH_{nucl} / kJmol ⁻¹	T_m / K	ΔG / kJmol ⁻¹	σ	χ^2
3 μ M; 652nm, absorbance	-153.81 \pm 6.63	- 384.5 \pm 20.7	0	316.0	-39.16	1	4.11 E-02
4 μ M; 652nm, absorbance	-147.53 \pm 5.27	-365.1 \pm 16.4	0	317.1	-38.67	1	2.64 E-02
5 μ M; 652nm, absorbance	-146.07 \pm 4.22	-364.1 \pm 13.1	0	316.0	-37.50	1	1.85 E-02
6 μ M; 652nm, absorbance	-161.10 \pm 7.29	- 408.1 \pm 22.6	0	318.8	-39.42	1	4.58 E-02
\emptyset	-151.63 \pm 5,85	-380,45 \pm 18.1	0		-38.69	1	

Method 2: Global fitting

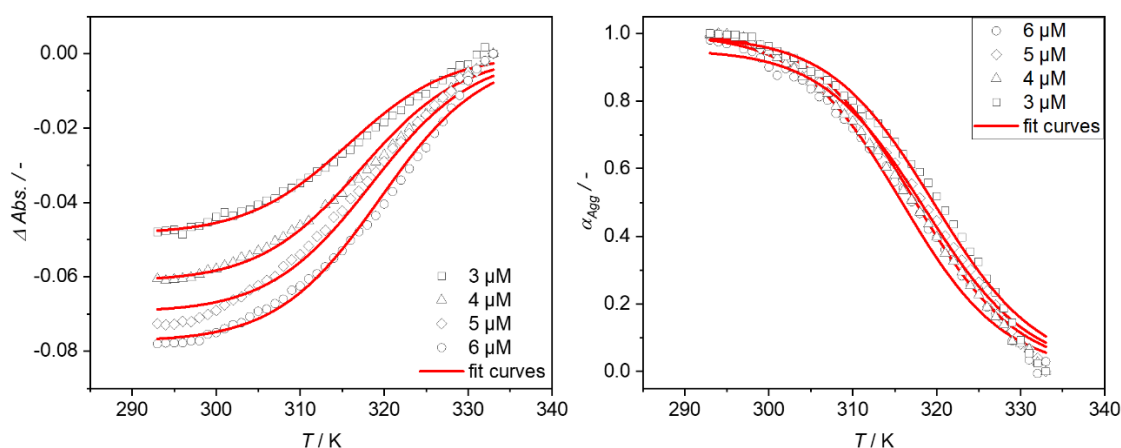


Figure S35. Global fit data obtained for different concentrations for the temperature-induced disassembly of **Agg2**. *Left:* Curves extracted from the absorption data. *Right:* Corresponding curves obtained for the degree of aggregation (α_{Agg}).

Table S2. Thermodynamic parameters derived from global fitting (heating **Agg 2**).

dataset	T_m / K	$\Delta G / \text{kJmol}^{-1}$	σ	χ^2
3 μM ; α_{Agg}	315.9	-38.7	1	2.02E-01
4 μM ; α_{Agg}	317.5	-38.7	1	2.02E-01
5 μM ; α_{Agg}	318.1	-38.7	1	2.02E-01
6 μM ; α_{Agg}	319.6	-38.7	1	2.02E-01

The given data implies an isodesmic self-assembly mechanism for the formation/disassembly of **Agg2**. Both approaches, either by individual fitting of the single concentrations and subsequent averaging or by fitting all concentrations simultaneously give a Gibbs free energy of $\Delta G = -38.7 \text{ kJ/mol}$.

Agg3 via cooling²

Method : Individual fits + averaging

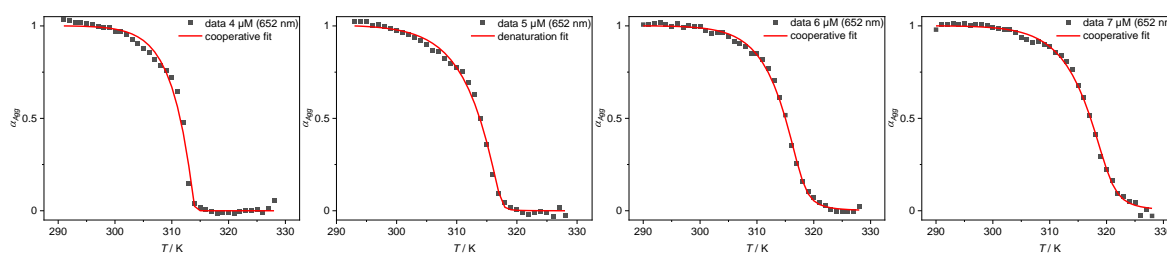


Figure S36. Plot of the degree of aggregation (α_{Agg}) against the temperature for different concentrations and corresponding individual fit curves obtained from the nucleation-elongation model for **Agg3**.

Table S3. Thermodynamic parameters derived from individual fitting to the nucleation-elongation model for **Agg3**.

dataset	$\Delta H^{298} /$ kJmol ⁻¹	$\Delta S^{298} /$ Jmol ⁻¹	$\Delta H_{\text{nucl}}^{298} /$ kJmol ⁻¹	$T_e /$ K	$\Delta G^{298} /$ kJmol ⁻¹	K_{el}	K_{nucl}	σ	χ^2
4 μ M; 652nm, ALPHA	-223.7 \pm 19.6	-609.1 \pm 63.0	-27.8 \pm 17.9	314.0	-42.1	250021.2	5.9	2.37e-05	3.65e-02
5 μ M; 652nm, ALPHA	-167.0 \pm 10.6	-425.1 \pm 33.8	-19.6 \pm 4.3	317.1	-40.2	200019.3	119.0	5.95e-04	1.67e-02
6 μ M; 652nm, ALPHA	-202.6 \pm 10.3	-538.5 \pm 32.9	-10.4 \pm 1.0	317.2	-42.0	166685.9	3252.2	1.95e-02	8.95e-03
7 μ M; 652nm, ALPHA	-182.3 \pm 10.6	-471.7 \pm 33.8	-9.7 \pm 1.0	319.6	-41.7	142857.5	3716.3	2.60e-02	1.20e-02
\emptyset	-193.9 \pm 12.8	-511.1 \pm 40.9	-16.9 \pm 6.1		-41.5				

The given data implies a cooperative self-assembly mechanism for the formation of **Agg3**. The averaged Gibbs free energy of -41.5 kJ/mol agrees well with **Agg3** being the most stable species.

7. FESEM images

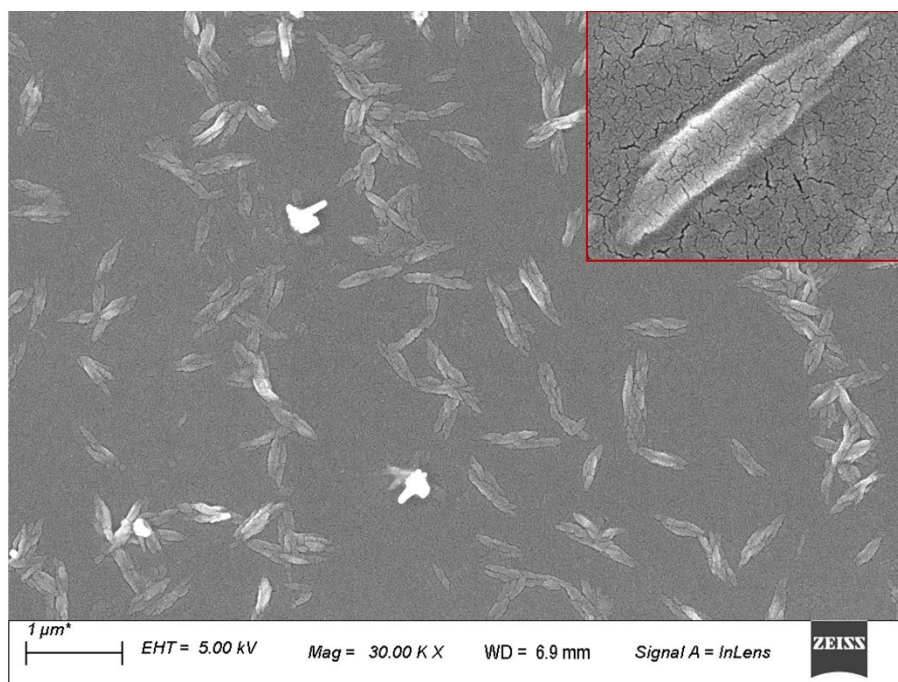


Figure S37. FESEM image of aggregate of PNIBF₂ in MCH/DCE (v/v = 99:1). Image was captured after drop-casting a solution of the aggregate. Zoomed view of **Agg1** is shown in inset.

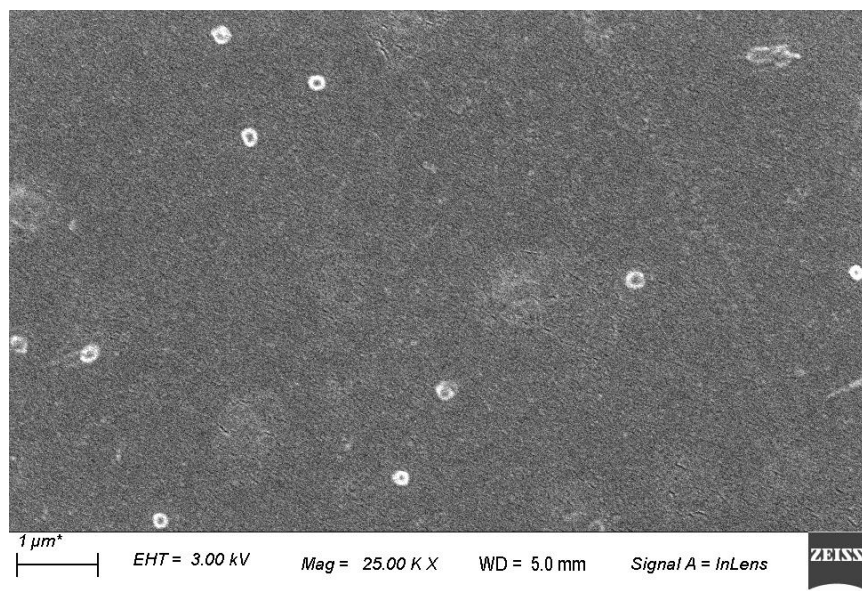


Figure S38. FESEM image of **Agg3** in water/THF (v/v = 76:24). Image was captured after drop-casting a solution of the aggregate.

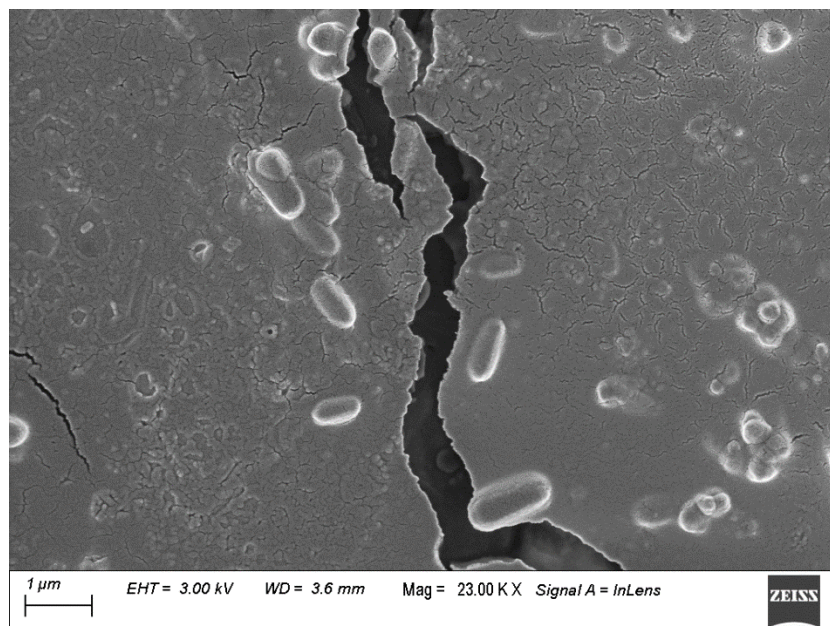


Figure S39. FESEM image of PNIBF₂ in water/THF (v/v = 95:5). Image was captured after drop-casting a solution of the aggregate.

8. References

- (1) R. J. Das and K Mahata, *Org. Lett.*, 2018, **20**, 5027-5031.
- (2) M. M. J. Smulders, M. M. L. Nieuwenhuizen, T. F. A. de Greef, P. van der Schoot, A. P. H. J. Schenning and E. W. Meijer, *Chem. Eur. J.*, 2010, **16**, 362-367.